International Geology Review, Vol. 46, 2004, p. 226–234.
Copyright © 2004 by V. H. Winston & Son, Inc. All rights reserved.

When Did the Emeishan Mantle Plume Activity Start? Geochronological and Geochemical Evidence from Ultramafic-Mafic Dikes in Southwestern China

FENG GUO,[1] WEIMING FAN, YUEJUN WANG, AND CHAOWEN LI

Key Laboratory of Marginal Sea Geology, Guangzhou Institute of Geochemistry and South Sea Institute of Oceanology, Chinese Academy of Sciences, Wushan, Guangzhou, 510640 China

Abstract

SHRIMP zircon U-Pb dating of an ultramafic-mafic dike intruded into Lower Devonian limestones from southwestern China gives a mean $^{238}U/^{206}Pb$ age of 262 ±3 Ma (n = 12, MEWD = 5.7). This is the oldest age hitherto reported for the Emeishan large igneous province (ELIP). These and related dikes have OIB-like trace-element signatures (e.g., low LILE/HFSE, LREE/HFSE, and Zr/Nb ratios) and strong geochemical and Sr-Nd isotopic similarities to the least contaminated ELIP high-Ti basalts. A compilation of published Ar/Ar and SHRIMP zircon U-Pb ages for the ELIP shows that plume activity probably started at ~262 Ma, and attained its maximum at 253–251 Ma as a result of continuous plume-lithosphere interaction. The ~10 m.y. interval of the ELIP magmatic episode favors a plume-impaction model, wherein the plume head impinged on the base of the lithosphere over a time scale predicted by laboratory experiments.

Introduction

MANTLE PLUMES and associated voluminous eruption of lavas are generally considered to be a potentially important cause for crises in global climate and biological extinction (e.g., Bowring et al., 1998; Courtillot et al., 1999; Olsen, 1999; Wignall, 2001). The Emeishan large igneous province (ELIP) was recently interpreted as the product of a mantle plume active at the Permo-Triassic time boundary in southwestern China (e.g., Chung and Jahn, 1995; Chung et al., 1998; Xu et al., 2001; Lo et al., 2002; Zhou et al., 2002). Due to the paucity of reliable age constraints and/or the prolonged duration of the magmatic activity in the ELIP, debate continues concerning the main eruption stages and temporal links with mass extinction events that occurred at the end of the Paleozoic Era (e.g., Erwin, 1994; Stanley and Yang, 1994). Zhou et al. (2002) conducted Sensitive High-Resolution Ion Microprobe (SHRIMP) zircon U-Pb dating on the Xinjie mafic intrusion, and derived a mean $^{238}U/^{206}Pb$ age of 259 ±3 Ma. They interpreted the age as representative of the main eruption event of the ELIP, and postulated a temporal link with the end-Guadalupian mass extinction event at 256–259 Ma (Stanley and Yang, 1994; Courtillot et al., 1999). Lo et al. (2002) performed high-precision Ar-Ar dating on volcanic and intrusive rocks of the ELIP, and reported a main eruption time scale of 251–253 Ma. This range is nearly synchronous with the Siberian large igneous province (LIP) of ~251 Ma (Renne et al., 1995; Kamo et al., 1996); Lo et al. (2002) inferred that both LIPs were related to the mass extinction event at the Permo-Triassic boundary.

It is usually considered that the eruption duration of a LIP spans several million years, with high eruptive rates of 0.1 to >1.0 km^3/yr (White and McKenzie, 1989, 1995; Hill, 1993; Campell and Griffiths, 1990; Griffiths and Campbell, 1990). In this respect, the aforementioned age range of ~ 5–8 m.y. for the main eruption ages of the ELIP might reflect magmatic episodes of different stages following plume impact. Thus a key issue for the debate is to constrain when the Emeishan plume activity started. Here, we used SHRIMP to analyze zircon from an ultramafic to mafic dike intruded into Lower Devonian limestones in Yanyuan County, southwestern China. A mean $^{238}U/^{206}Pb$ age of 262 ± 3 Ma (n = 12, MEWD = 5.7) was obtained. These rocks have OIB-type trace-element and isotopic signatures, and exhibit remarkable similarities to the least contaminated Emeishan high-Ti basalts (Xu et al., 2001), suggesting that they were products of the same plume source as that tapped by the high-Ti basalts.

[1]Corresponding author; email: guofengt@263.net

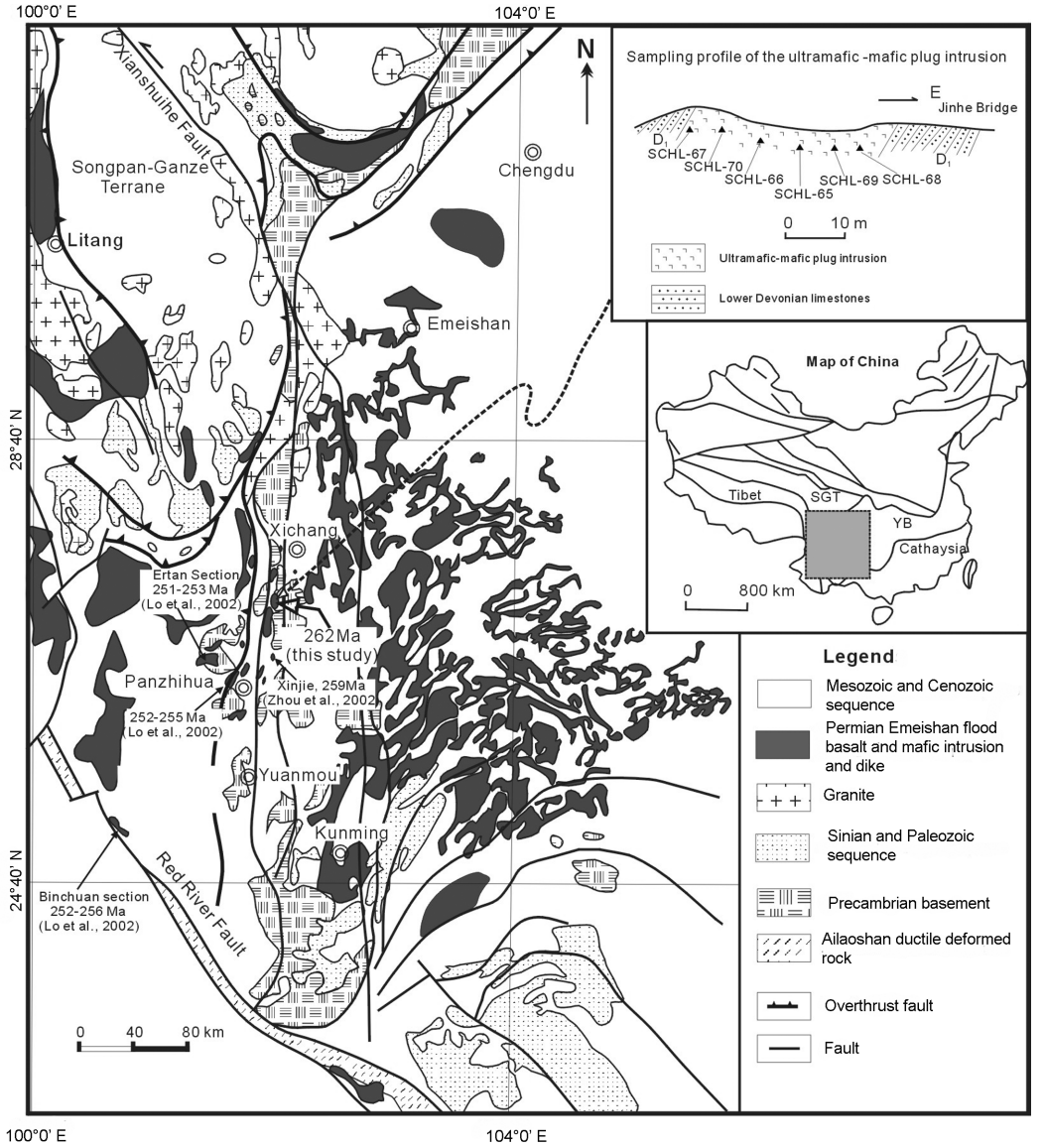

FIG. 1. Distribution of the Emeishan flood basalts and associated mafic intrusions in southwestern China (modified after Lin, 1985; Zhou et al., 2002). The upper right inset shows the sampling profile of the ultramafic-mafic plug intrusion. Abbreviations: SGT= Songpan-Ganze Terrane; YB= Yangtze Block.

Petrologic Features of Ultramafic-Mafic Dikes

Permian flood basalts are widely distributed in southwestern China, especially in Yunan, Guizhou, and Sichuan provinces (Lin, 1985, Fig. 1). These basalts are regarded as products of the Emeishan plume (Chung and Jahn, 1995; Chung et al., 1998; Xu et al., 2001). Besides the flood basalts, numerous ultramafic-mafic intrusions and dikes occur in the region (SBGMR, 1991, Fig. 1). The tabular intrusives occur as dikes, sills, and plugs. Most are closely associated with the Emeishan flood basalts (e.g., Xinjie intrusion, Zhou et al., 2002); a few

dikes were intruded into sedimentary rocks such as Devonian–Carboniferous limestones and sandstones (SBGMR, 1991). The ages of most of these dikes are still unknown, and some may provide evidence for the earliest magmatic episodes associated with plume impact on the lithosphere.

The ultramafic-mafic dike described in this paper occurs in Yanyuan County of the Panxi paleorift, southwestern China. It is intruded into Lower Devonian limestones, with a width of about 35 m (Fig. 1). The studied samples are coarse-grained noritic olivine gabbros (8–30 mm grain size) with a phase assemblage including olivine (5–20%), orthopyroxene (10–25%), clinopyroxene (30–45%), plagioclase (30–40%), and accessory ilmenite, zircon, and apatite. The rocks are unmetamorphosed and zones of olivine cumulate enrichment are well developed, as indicative of significant crystal fractionation before emplacement.

Sample Preparation and Analytical Techniques

Zircon for SHRIMP U-Pb dating was separated from sample No. SCHL-66, a coarse-grained olivine gabbro. Prior to chipping, the sample weighed about 30 kg; it was crushed into chips of 1–2 cm grain size and then ground to < 0.1 mm in an agate mill. Zircon was handpicked under a binocular microscope after segregation by conventional heavy liquid and electron-magnetic techniques. The zircon grains were mounted in epoxy resin, polished, and coated with gold. The mount was then photographed in transmitted and reflected light using cathodoluminescence images for identification of the analyzed grains. U-Pb isotope analysis was conducted with a SHRIMP II at the Beijing Ion Microprobe Center, Chinese Academy of Geological Sciences. The analytical technique used here was similar to that described by Compston et al. (1984, 1992) and Williams and Claesson (1987). Correction of the common Pb contribution followed the ^{204}Pb method of Compston et al. (1984) and a common Pb composition of Cumming and Richards (1975). Age uncertainties quoted below are at the 2σ level. Decay constants used are those recommended by Steiger and Jager (1977). The U-Pb dating results for zircon are listed in Table 1.

Major oxide compositions were determined at Hubei Institute of Geology and Mineral Resources, Ministry of Land and Resources, employing wavelength X-ray fluorescence spectrometry (XRF) with analytical errors <2%. Trace-element ICP-MS analysis was carried out at the Guiyang Institute of Geochemistry, Chinese Academy of Sciences (CAS). Detailed description of the analytical technique employed and analytical errors were reported in Qi et al. (2000). Sr and Nd isotopic ratios were measured at the Institute of Geology and Geophysics, CAS. Rock chips <20 mesh grain size were used for Sr and Nd isotope analysis. Before being ground to <160 mesh and chemical dissolution, these chips was leached by purified 6N HCl for 24 hours at room temperature to remove the influence of surface alteration or weathering. The Sr and Nd isotopic ratios were normalized to $^{86}Sr/^{88}Sr = 0.1194$ and $^{146}Nd/^{144}Nd = 0.7219$, respectively. The La Jolla standard yielded $^{143}Nd/^{144}Nd = 0.511862 \pm 12$ ($n = 10$) and the NBS987 standard gave $^{87}Sr/^{86}Sr = 0.710240 \pm 10$ ($n = 6$). The whole procedure blank ranges from 2 to 5×10^{-10}g for Sr and less than 5×10^{-11}g for Nd. The analytical errors for Sr and Nd isotopic ratios are given as 2σ. Major- and trace-element compositions and Sr-Nd isotope data of the samples are listed in Table 2.

Results

Emplacement age of the ultramafic-mafic dike

Fifteen zircon grains were analyzed, which give an apparent $^{238}U/^{206}Pb$ age range from 244 to 273 Ma. Zircon (grain 10) has the youngest apparent $^{238}U/^{206}Pb$ age (244 Ma), and plots away from the concordia curve as a result of radiogenic Pb loss. Grain 6 shows a reasonable $^{238}U/^{206}Pb$ age (264 Ma), but plots even farther away from the concordia curve due to exotic ^{207}Pb addition; thus this point is not suitable for age calculation. Grain 13, which is a high-U zircon with Th/U of 0.88, has also not been employed in the age calculation. The remaining 12 zircon grains that plot near or on the concordia line give a mean $^{238}U/^{206}Pb$ age of 262 ±3 Ma with MSWD value of 5.7 ($n = 12$) (Fig. 2), which represents the crystallization age of the intrusion. This is the oldest emplacement age of magmas related to the ELIP.

Geochemical characteristics

From Table 2, it can be seen that the samples from the margin to the center of the intrusion span a large range in MgO (MgO = 8.38–21.33%) and TiO_2 (1.04–1.75%). Because they are olivine, pyroxene, and plagioclase cumulates, these rocks have low incompatible-element concentrations (e.g., LILE,

TABLE 1. U-Th-Pb SHRIMP Analytical Results for Zircon Grains of an Ultramafic Dike (SCHL-66) from Yanyuan, Southwestern China[1]

Grain	Concentration, ppm				Calculation ratios						Calculated ages, Ma					
	U	Th	Pb	Th/U	207/206	±	206/238	±	207/235	±	206/238	±	208/232	±	207/206	±
1	1166	2806	40.8	2.49	0.05129	0.0005	0.04070	0.0005	0.2851	0.0046	257	4	258	4	232	23
2	2028	2430	73.1	1.24	0.05151	0.0004	0.04195	0.0005	0.2991	0.0045	265	4	260	4	273	18
3	1952	3355	71.4	1.78	0.05118	0.0004	0.04254	0.0005	0.2967	0.0044	269	4	273	4	222	19
4	4205	7187	153	1.77	0.05332	0.0005	0.04240	0.0002	0.3029	0.0039	268	2	251	2	277	28
5	2681	7202	96.1	2.78	0.05426	0.0007	0.04161	0.0002	0.2997	0.0054	263	2	247	2	296	39
6	253	221	9.21	0.90	0.08080	0.0032	0.04171	0.0005	0.3940	0.0307	263	4	281	14	882	160
7	1991	2547	69.8	1.32	0.05339	0.0008	0.04072	0.0003	0.2929	0.0050	257	2	246	3	293	35
8	1860	2409	66.6	1.34	0.05350	0.0012	0.04158	0.0002	0.2934	0.0091	263	2	258	3	248	71
9	1040	2440	36.4	2.42	0.05300	0.0010	0.04072	0.0003	0.2929	0.0062	257	2	258	3	292	45
10	872	3510	28.9	4.16	0.05480	0.0011	0.03855	0.0002	0.2876	0.0072	244	2	248	3	376	53
11	3197	3983	118	1.29	0.05365	0.0005	0.04282	0.0003	0.3088	0.0043	270	2	271	3	298	31
12	1279	1310	45.2	1.06	0.05594	0.0009	0.04102	0.0002	0.3062	0.0073	259	3	248	4	376	50
13	3105	2641	116	0.88	0.05459	0.0006	0.04325	0.0002	0.3166	0.0047	273	2	267	3	333	32
14	1451	2405	51.2	1.71	0.05546	0.0008	0.04093	0.0002	0.2959	0.0068	259	2	249	3	305	51
15	2281	2779	84.9	1.26	0.05432	0.0009	0.04319	0.0002	0.3081	0.0074	272	2	257	3	274	53

[1]Errors are 1σ. The calculated $^{206}Pb/^{238}Pb$ ages are corrected using measured ^{204}Pb. Error in standard calibration was 0.79% (not included in above errors but required when comparing data from different mounts).

TABLE 2. Major-Oxide, Trace-Element, and Sr-Nd Isotopic Compositions of Ultramafic to Mafic Dikes from Yanyuan, Southwestern China

Sample:	SCHL-67	SCHL-65	SCHL-66	SCHL-68	SCHL-69	SCHL-70	EM-42	EM-48
Rock type:	Mafic dike	Ultramafic dike	Ultramafic dike	Mafic dike	Ultramafic dike	Mafic dike	High-Ti basalt	High-Ti basalt
Reference:	This study						Xu et al., 2001	
SiO_2	46.32	43.84	45.37	45.6	45.28	47.08	46.96	45.71
TiO_2	1.46	1.50	1.08	1.75	1.04	1.69	4.00	4.13
Al_2O_3	15.71	7.97	6.35	10.22	5.80	8.66	12.82	13.05
Fe_2O_3	3.35	3.50	1.57	3.14	1.96	3.23	15.99	16.40
FeO	7.83	8.52	10.83	7.97	9.63	6.63		
CaO	11.64	8.34	10.94	14.15	12.27	15.13	10.68	9.12
MgO	8.38	20.68	20.31	12.77	21.33	13.07	5.06	5.18
MnO	0.17	0.17	0.20	0.16	0.19	0.16	0.21	0.28
K_2O	0.41	0.36	0.22	0.17	0.14	0.28	0.55	0.60
Na_2O	1.75	1.14	1.28	1.84	0.85	1.76	2.23	3.30
P_2O_5	0.12	0.13	0.11	0.11	0.06	0.14	0.42	0.43
LOI	2.64	3.49	1.49	1.85	1.18	1.87	1.04	1.73
Total	99.78	99.64	99.75	99.73	99.73	99.7	99.96	99.93
Mg#	0.58	0.76	0.75	0.68	0.77	0.71	0.39	0.39
Cr	104	1520	1219	862	2611	1763	98	91
Ni	135	902	486	206	496	297	77	76
Rb	11.1	12.2	4.9	2.4	3.1	8.1	10	8
Sr	277	254	159	254	128	267	419	408
Ba	99	125	86	90	66	217	219	286
Nb	8.2	12.5	8.5	10.0	5.2	13.9	34	34
Ta	0.51	0.81	0.49	0.62	0.34	0.86	2.1	1.9
Th	0.67	1.62	0.75	0.75	0.49	1.21	3.9	3.7
U	0.19	0.37	0.22	0.12	0.12	0.28	0.9	0.9
Zr	71.9	98.4	62.1	75. 6	46.5	92.3	257	252
Hf	2.32	3.12	2.09	2.88	1.88	3.22	6.8	6.4
Y	16.4	14.7	13.0	18.4	12.5	17.3	43	42
La	7.68	12.24	7.45	8.36	4.79	11.81	33.7	31.7
Ce	18.69	28.97	17.24	21.39	12.48	28.23	74.4	68.7
Nd	11.51	16.34	10.82	14.39	8.96	17.84	45	40.4
Sm	3.33	3.81	2.97	4.24	2.64	4.46	9.79	8.89
Eu	1.06	1.09	0.89	1.22	0.80	1.31	3.1	2.81
Tb	0.56	0.55	0.44	0.62	0.45	0.67	1.36	1.23
Yb	1.48	1.22	1.16	1.40	1.05	1.43	3.20	3.52
Lu	0.21	0.18	0.16	0.19	0.15	0.20	0.46	0.44
$^{87}Sr/^{86}Sr \pm 2\sigma$		0.704901 ± 14	0.704080 ± 8			0.704169 ± 10	0.704178 ± 8	0.704565 ± 10
$^{87}Sr/^{86}Sr(i)$		0.70438	0.70375			0.70384	0.70393	0.70436
$^{143}Nd/^{144}Nd \pm 2\sigma$		0.512778 ± 8	0.512848 ± 6			0.512810 ± 5	0.512779 ± 5	0.512768 ± 5
$\varepsilon_{Nd}(t)$		+4.6	+5.1			+4.9	+4.9	+4.6

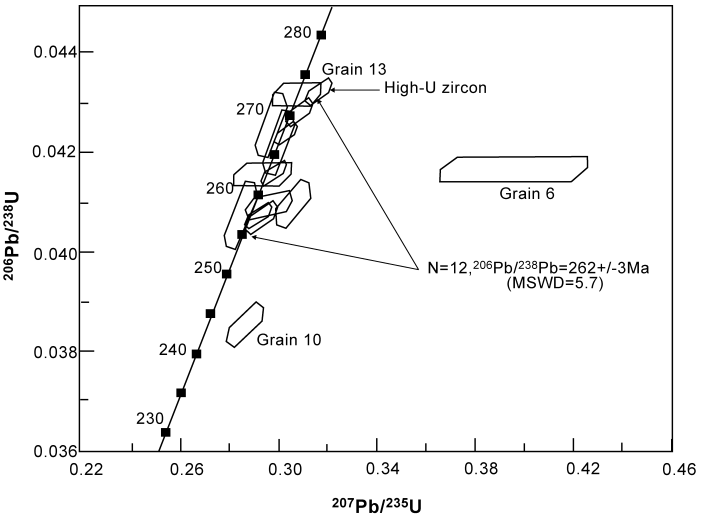

FIG. 2. Concordia plots of the SHRIMP zircon results of an ultramafic dike sample (SCHL-66), giving a mean $^{238}U/^{206}Pb$ age of 262 ± 3 Ma (n =12; MSWD = 5.7), representing the crystallization age of the intrusion.

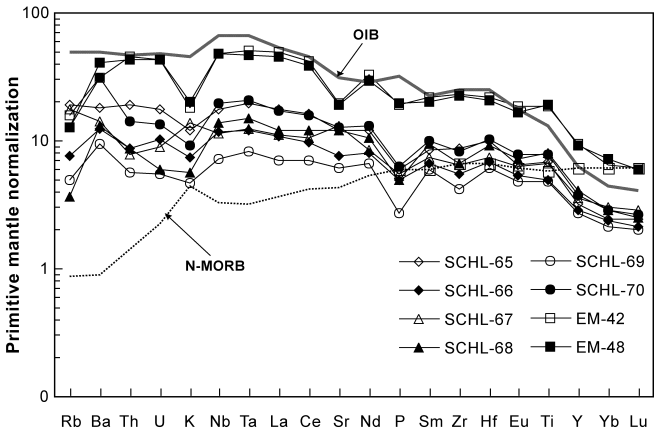

FIG. 3. Primitive mantle–normalized spidergrams of the ultramafic-mafic dikes in southwestern China. Note that both the ultramafic-mafic dikes and the least contaminated high-Ti basalts from the ELIP show similar multi-element patterns, suggesting a common origin for both types of rocks. Data sources: EM-42 and EM-48 are the least contaminated high-Ti basalts (Xu et al., 2001); PM, OIB, and N-MORB are from Sun and McDonough (1989).

LREE, and HFSE) but high concentrations of compatible elements like Cr and Ni relative to the Emeishan high-Ti basalts (Xu et al., 2001). In essence, they show clear OIB-type trace-element signatures—e.g., low La/Nb (0.84–0.98), Zr/Nb (7.3–7.8), Ba/Nb (9.1–15.7), and Th/Nb (0.08–0.13) (Weaver, 1991)—very similar to those of the least contaminated high-Ti basalts in the ELIP (Table 2; Xu et al., 2001). A spidergram is presented in Figure 3.

The ultramafic-mafic dikes have a very limited range in Nd isotopic ratios but a relatively larger range in Sr isotopic compositions. The age-corrected $\varepsilon_{Nd}(t)$ value has a range from +4.6 to +5.1, and an

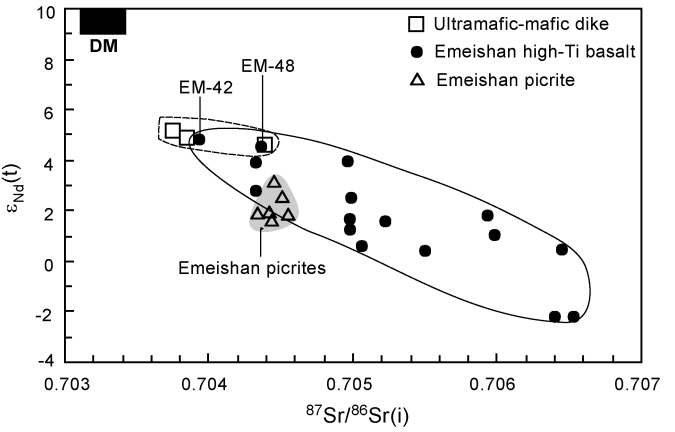

FIG. 4. Sr-Nd isotope variation diagram of the ultramafic-mafic dikes and comparison with the contemporaneous mafic rocks from the ELIP. Data sources: Emeishan high-Ti flood basalts (Xu et al., 2001); Emeishan picrites (Chung et al., 1998).

initial $^{87}Sr/^{86}Sr(i)$ range of 0.70375 to 0.70438 (Table 2 and Fig. 4), overlapping the range of the least-contaminated Emeishan high-Ti flood basalts reported by Xu et al. (2001). The strong geochemical and isotopic similarities between the ultramafic-mafic dikes and the least contaminated high-Ti flood basalts probably indicate a common origin for both kinds of rocks.

Discussion

Geochemical evidence for mantle plume origin of the ultramafic-mafic dikes

Petrological, geochemical, and isotopic data of picrites, flood basalts, and associated intrusive rocks have revealed that the ELIP was derived from a mantle plume (e.g., Chung and Jahn, 1995; Chung et al., 1998; Xu et al., 2001). Among these rocks, the high-Ti basalts were considered to have been generated by relatively lower degrees of melting of a plume source that had ε_{Nd}= +5 and $^{87}Sr/^{86}Sr(i)$ of ~0.704 within the garnet stability field (Xu et al., 2001). Xu et al. (2001) further interpreted the geochemical variations in the high-Ti basalts as a result of shallow-level gabbroic fractionation and/or crustal contamination *en route* to the surface. It is therefore reasonable to attribute the OIB-type trace-element and Sr-Nd isotopic characteristics in the ultramafic-mafic dikes to the same plume source derivation as the high-Ti basalts. Also, due to the minor effect of fractional crystallization on MREE/HREE fractionation, Sm/Yb ratios can be indicative of the depth of melting (e.g., McKenzie and O'Nions, 1991). Hence the very similar Sm/Yb ratios between the ultramafic-mafic dikes (Sm/Yb = 2.3–3.1) and the least contaminated high-Ti basalts (Sm/Yb = 2.5–3.1) might suggest that both kinds of rocks were derived from similar melting depths (e.g., initially within the stability field of garnet).

Timing of the Emeishan LIPs and implications for plume ascent

An upwelling mantle plume transfers tremendous heat supply and mass to the Earth's surface (e.g., Griffiths and Campell, 1991; McKenzie and Bickle, 1988; White and McKenzie, 1989; Xu et al., 2001). Plume-lithosphere interaction at different depths will produce a wide spectrum of basaltic rocks of compositional heterogeneity, such as picrites, high-Ti and low-Ti flood basalts, and ultramafic-mafic intrusions. In the ELIP, apart from the main age spectrum mentioned above, Lo et al. (2002) also reported that biotite separates from a mafic intrusion gave an Ar-Ar age of 255 Ma. A compilation of recent SHRIMP zircon U-Pb and reliable Ar-Ar ages shows that the ELIP includes at least the following magmatic episodes: (1) the earliest ultramafic-mafic dikes at ~262 Ma; (2) the mafic intrusions of 255–259 Ma (Lo et al., 2002; Zhou et

al., 2002); and (3) the latest eruption of the flood basalts at 251–253 Ma (Lo et al., 2002).

The onset of the plume head at the lithosphere's base would have resulted in lithospheric extension, and may firstly have produced melts like the earliest ultramafic-mafic dikes once the geotherm crossed the peridotite solidus temperature(e.g., McKenzie and Bickle, 1988). As plume ascent continued, stronger extension, crustal stretching, and larger degrees of melting of plume and/or the lithospheric mantle occurred to form the mafic intrusions. Finally, the split-up of the lithosphere (e.g., the formation of the Panxi paleorift) and the strongest impact on the lithosphere caused the voluminous eruption of continental flood basalts (Yuan et al., 1985). It seems likely that the ultramafic-mafic dikes, mafic intrusions, and the flood basalts in the ELIP well document the impact of the plume on the lithospheric evolution of southwestern China.

Although debate continues about the time interval between arrival of the plume head at the base of the lithospheric mantle, and the eruption of a large amount of magmas (e.g., Campbell and Griffiths, 1990; Kent et al., 1992), geochronological evidence from most LIPs tends to suggest that voluminous volcanism occurred relatively quickly (several to ten million years) after the plume head impinged on the base of the lithosphere, such as in the Siberian, Deccan, and the North Atlantic large igneous provinces (Kerr, 1994; Renne et al., 1995; Kamo et al., 1996; Allègre et al., 1999). Therefore, the ~10 m.y. (from 262 to 253–251 Ma) time interval of the magmatic episode for the ELIP favors a plume-impaction model, consistent with the time scale suggested by laboratory experiments (e.g., Campbell and Griffiths, 1990; Hill, 1993).

Conclusions

SHRIMP zircon U-Pb dating results of an ultramafic-mafic dike intruded into Lower Devonian limestones from southwestern China show that the earliest magmatic record in the ELIP is at least as old as 262 Ma; this age might represent the initiation of Emeishan plume activity. The OIB-like trace-element signatures in these rocks, and remarkable trace-element and isotopic similarities to the least contaminated Emeishan high-Ti basalts, indicate that they were derived from the same plume source as that documented by the high-Ti basalts. Considering the reliable age spectrum of the ELIP (from 262 Ma to 251–253 Ma), it is reasonable to conclude that the mafic rocks (including the intrusive and extrusive rocks) in the ELIP were the products of plume-lithosphere interaction following plume impaction.

Acknowledgments

Thanks are due to Prof. D. Y. Liu and Dr. P. Jian for technical help during analysis of zircon on SHRIMP II. Prof. Richard Arculus is appreciated for his helpful suggestions and assistance with English exposition. This study was financially supported by the National Ministry of Science and Technology of China (G1999043205) and the Chinese Academy of Sciences (KXCZ2-101).

REFERENCES

Allègre, C. J., Birck, J. L., Capmas, F., and Courtillot, V., 1999, Age of the Deccan traps using ^{187}Re-^{187}Os systematics: Earth and Planetary Science Letters, v. 170, p. 197–204.

Bowring, S. A., Erwin, D. H., Jin, Y. G., Martin, M. W., Davidek, K., and Wang, W., 1998, U/Pb zircon geochronology and tempo of the end-Permian mass extinction: Science, v. 280, p. 1039–1045.

Campbell, I. H., and Griffiths, R. W., 1990, Implications of mantle plume structure for the evolution of flood basalts: Earth and Planetary Science Letters, v. 99, p. 79–93.

Compston, W., Williams, I. S., and Meyer, C., 1984, U-Pb geochronology of zircons from Lunar Breccia 73217 using a sensitive high mass resolution ion microprobe: Journal of Geophysical Research, v. 89, p. 525–534.

Compston, W., Williams, I. S., Kirschvink, J. L., Zhang, Z. C., and Ma, G. G., 1992, Zircon U-Pb ages for the Early Cambrian time scale: Journal of the Geological Society of London, v. 149, p. 171–184.

Chung, S. L., and Jahn, B. M., 1995, Plume-lithosphere interaction in generation of the Emeishan flood basalts at the Permian–Triassic boundary: Geology, v. 23, p. 889–892.

Chung, S. L., Jahn, B. M., Wu, G., Lo, C. H., and Cong, B., 1998, The Emeishan flood basalt in SW China: A mantle plume initiation model and its connection with continental breakup and mass extinction at the Permian–Triassic boundary, *in* Flower, M. F. J., Chung, S. L., Lo, C. H., and Lee, T. Y., eds., Mantle dynamics and plate interaction in East Asia: Geodynamics, v. 27, p. 47–58.

Courtillot, V., Jaupart, C., Manighetti, I., Tapponnier, P., and Basse, J., 1999, On causal links between flood basalts and continental breakup: Earth and Planetary Science Letters, v. 166, p. 177–195.

Cumming, G. L., and Richards, J. R., 1975, Ore lead isotope ratios in a continuously changing Earth: Earth and Planetary Science Letters, v. 28, p. 155–171.

Erwin, D. H., 1994, The Permo-Triassic extinction: Nature, v. 367, p. 231–236.

Griffiths, R. W., and Campbell, I. H., 1990, Stirring and structure in mantle plumes. Earth and Planetary Science Letters, v. 99, p. 66–78.

_____, 1991, Interaction of mantle plume heads with the Earth's surface and onset of small-scale convection: Earth and Planetary Science Letters, v. 103, p. 214–227.

Hill, R. I., 1993, Mantle plumes and continental tectonics: Lithos, v. 30, p. 193–206.

Kamo, S. L., Czamanske, G. K., and Krögh, T. E., 1996, A minimum U-Pb age of the Siberian flood-basalt volcanism: Geochimica et Cosmochimica Acta, v. 60, p. 3505– 3511.

Kent, A. C., Kempton, P. D., and Saunders, A. D., 1992, Large igneous provinces: Sites of plume impact or plume incubation?: Geology, v. 20, p. 891–894.

Kerr, A., 1994. Lithospheric thinning during the evolution of continental large igneous provinces: A case study from North Atlantic Tertiary province: Geology, v. 22, 1027–1039.

Lin, J. Y., 1985, Spatial and temporal distribution of Emeishan basaltic rocks in the three southwestern provinces (Sichuan, Yunnan, and Guizhou) of China: China Science Bulletin, v. 30, p. 929–932 (in Chinese).

Lo, C. H., Chung, S. L., Lee, T. Y., and Wu, G., 2002, Age of the Emeishan flood magmatism and relations to Permian–Triassic boundary events: Earth and Planetary Science Letters, v. 198, p. 449–458.

McKenzie, D. P., and Bickle, M. J., 1988, The volume and composition of melt generated by extension of the lithosphere: Journal of Petrology, v. 32, p. 625–679.

McKenzie, D. P., and O'Nions, R. K., 1991, Partial melt distribution of melt generated by rare earth element concentrations: Journal of Petrology, v. 21, p. 1021–1091.

Olsen, P. E., 1999, Giant lava flows, mass extinctions, and mantle plumes: Science, v. 284, p. 604–605.

Qi, L., Hu, J., and Grégoire, D.C., 2000, Determination of trace elements in granites by inductively coupled plasma mass spectrometry: Talanta, v. 51, p. 507–513.

Renne, P. R., Zhang, Z. C., Richards, M. A., Black, M. T., and Basu, A. R., 1995, Synchrony and causal relations between Permian–Triassic boundary crises and Siberian flood volcanism: Science, v. 269, p. 1413–1416.

SBGMR (Sichun Bureau of Geology and Mineral Resources), 1991, Regional Geology of Sichun Province: Beijing, China, Geological Publishing House, 680 p. (in Chinese).

Stanley, S. M., and Yang, X., 1994, A double mass extinction at the end of the Paleozoic era: Science, v. 266, p. 1340–1344.

Steiger, R. H., and Jager, E., 1977, Subcommission on geochronology: Convention on the use of decay constants in geo- and cosmo-chronology: Earth and Planetary Science Letters, v. 36, p. 359–362.

Sun, S. S., and McDonough, W. F., 1989, Chemical and isotopic systematics of oceanic basalts: Implication for mantle composition and processes, *in* Saunders, A. D., and Norry, M. J., eds., Magmatism in the ocean basins: Geological Society of London Special Publication, v. 42, p. 313–345.

Weaver, B. L., 1991, The origin of ocean island basalts end-member composition: Trace element and isotopic constraints: Earth and Planetary Science Letters, v. 104, p. 381–397.

White, R. S., and McKenzie, D. P., 1989, Magmatism at rift zones: The generation of continental margins and flood basalts: Journal of Geophysical Research, v. 94, p. 7685–7729.

_____, 1995, Mantle plume and continental flood basalts: Journal of Geophysical Research, v. 100, p. 17,543–17,585.

Wignall, P. B., 2001, Large igneous provinces and mass extinctions: Earth Science Review, v. 53, p. 1–33.

Williams, I. S., and Claesson, S., 1987, Isotopic evidence for the Precambrian provenance and Caledonian metamorphism of high-grade paragneisses from the Deve Nappes, Scandinavian Caledonides (II): Ion microprobe zircon U-Th-Pb: Contributions to Mineralogy and Petrology, v. 97, p. 205–217.

Xu, Y. G., Chung, S. L., Jahn, B. M., and Wu, G. Y., 2001, Petrological and geochemical constraints on the petrogenesis of Permian–Triassic Emeishan flood basalts in southwestern China: Lithos, v. 58, p. 145–168.

Yuan, H. H., Zhang, S. F., Zhang, P., Liu, D., Shi, Z. M., Shen, F. K., Zhou, F. B., and Wang, M. K., 1985, Isotopic geochronology of the magmatic rocks in Panxi paleorift: Beijing, China, Geological Publishing House, p. 241–257 (in Chinese).

Zhou, M. F., Malpas, J., Song, X. Y., Robinson, P. T., Sun, M., Kennedy, A. K., Lesher, C. M., and Keays, R. R., 2002, A temporal link between the Emeishan large igneous province (SW China) and the end-Guadalupian mass extinction: Earth and Planetary Science Letters, v. 196, p. 113–122.